

Neutrino mediated muon–electron conversion in nuclei revisited

F. Šimkovic ^{*}, V.E. Lyubovitskij, Th. Gutsche, Amand Faessler

Institut für Theoretische Physik, Universität Tübingen, Auf der Morgenstelle 14, D-72076

Tübingen, Germany

Sergey Kovalenko [†]

Departamento de Física, Universidad Técnica Federico Santa María, Casilla 110-V, Valparaíso,

Chile

Abstract

The non-photonic neutrino exchange mechanism of the lepton flavor violating muon–electron conversion in nuclei is revisited. First we determine the nucleon coupling constants for the neutrino exchange mechanism in a relativistic quark model taking into account quark confinement and chiral symmetry requirements. This includes a new, previously overlooked tree-level contribution from neutrino exchange between two quarks in the same nucleon. Then for the case of an additional sterile neutrino we reconsider the coherent mode of this process. The presence of a mixed sterile-active neutrino state ν_h heavier than the quark confinement scale $\Lambda_c \sim 1$ GeV may significantly improve the prospects for observation of this process in future experiments as compared to the conventional scenario with only light neutrinos. Turning the arguments around we derive new experimental constraints on $\nu_h - \nu_{e,\mu}$ mixing from the

^{*}On leave of absence from Department of Nuclear Physics, Comenius University, Mlynská dolina F1, SK–842 15 Bratislava, Slovakia

[†]On leave of absence from the Joint Institute for Nuclear Research, Dubna, Russia

non-observation of muon–electron conversion.

The recent results from the Super-Kamiokande [1] and SNO [2] experiments on atmospheric and solar neutrinos give convincing evidence on neutrino oscillation and hence on neutrino masses and lepton flavor violation (LFV). As is known, experimental searches for rare processes offer complimentary information on the LFV. This can shed additional light on the physics underlying this phenomenon, discriminating various models beyond the standard model (SM) (for a review see [3]). The muon–electron $[(\mu^-, e^-)]$ conversion in nuclei [3–8],

$$\mu_b^- + (A, Z) \rightarrow (A, Z) + e^-, \quad (1)$$

is one of the most prominent lepton flavor changing reaction. Experiments searching for this process in the coherent channel with a monoenergetic final state electron have reached an unprecedented level of sensitivity. Presently, the most stringent upper limits on the branching ratio $R_{\mu e}$ related to the (μ^-, e^-) conversion has been set by the SINDRUM II collaboration [9]:

$$R_{\mu e} = \frac{\Gamma_{\mu e}}{\Gamma_{\mu\nu\mu}} < 6.1 \times 10^{-13} \quad (\text{target} : {}^{48}\text{Ti}), \quad 2.0 \times 10^{-11} \quad (\text{target} : {}^{79}\text{Au}), \quad (2)$$

where $\Gamma_{\mu e}$ and $\Gamma_{\mu\nu\mu}$ are the rates of the (μ^-, e^-) conversion and ordinary muon capture, respectively. Future experiments will significantly improve these limits. There are proposals of the SINDRUM II collaboration to reduce the current limits on the ratio $R_{\mu e}$ for ${}^{48}\text{Ti}$ and ${}^{197}\text{Au}$ down to 10^{-14} and 6×10^{-13} [9], respectively. A new Muon Electron COntversion (MECO) experiment on ${}^{27}\text{Al}$ is planned at BNL [10] with an expected sensitivity on the branching ratio of about 2×10^{-17} . Another future project PRIME [11] for the (μ^-, e^-) conversion on ${}^{48}\text{Ti}$ is going to reach a sensitivity of 10^{-18} . The realization of these projects would allow to set new stringent constraints on the LFV interactions relevant for the (μ^-, e^-) conversion. This process can be triggered by the LFV interactions associated with the exchange of neutrinos and/or new heavy particles (neutralinos, charginos, leptoquarks etc.) predicted in models beyond the SM [3–7]. In general all the (μ^-, e^-) conversion mechanisms

can be separated into photonic and non-photonic ones. A mechanism is photonic if it involves a virtual photon line connecting the effective leptonic LFV current with the electromagnetic nuclear current, otherwise a mechanism is non-photonic. These classes of mechanisms differ significantly on their particle and nuclear physics sides and are usually studied independently.

In this letter we concentrate on the non-photonic neutrino exchange mechanism. We are studying a model with three left-handed, weak doublet neutrinos $\nu'_{Li} = (\nu'_{Le}, \nu'_{L\mu}, \nu'_{L\tau})$ and a certain number n of the SM singlet, right-handed sterile neutrinos $\nu'_{Ri} = (\nu'_{R1}, \dots, \nu'_{Rn})$. Due to mixing they form $n + 3$ neutrino mass eigenstates N_i with masses m_i related to the weak eigenstates $\nu'_\alpha = (\nu'_{Le}, \nu'_{L\mu}, \nu'_{L\tau}, \nu'_{R1}, \dots, \nu'_{Rn})$ by an unitary mixing matrix U as $N_i = U_{\alpha i}^* \nu'_\alpha$.

Among N_i there must be at least three observable light neutrinos dominated by the active $\nu'_{e,\mu,\tau}$ components while the other states may be of arbitrary mass. In particular, they may include additional light neutrinos (ν_i), one of which might be relevant for the phenomenology of neutrino oscillations, as well as intermediate and heavy mass neutrinos (ν_h). The presence or absence of these neutrino states is an issue for experimental searches. For simplicity we consider the (ν_i, ν_h) scenario with an arbitrary number of light neutrinos ν_i with masses m_{ν_i} on the eV scale and one neutrino state ν_h with mass m_h larger than the typical hadronic scale $\Lambda_c \sim 1$ GeV. A similar scenario, but with ν_h having a mass below 1 GeV was previously studied in connection with K^\pm and τ semileptonic decays [12].

The analysis of the nuclear (μ^-, e^-) conversion starts with the elementary nucleon process $\mu^- + N \rightarrow N + e^-$. In models with non-trivial neutrino mixing this process can be realized at the quark level according to the diagrams of Fig. 1. The diagrams of Fig. 1a,b are the well-known one-quark box diagrams [3] while that of Fig. 1c is the new tree-level two-quark diagram. These lowest order diagrams represent the complete set of the neutrino exchange diagrams on quark-level relevant for the above nucleon process.

In the process considered the typical momentum transfer Q^2 to the nucleon is small comparable to the scale set by the muon mass with $Q^2 \sim m_\mu^2$. Therefore, the quarks in the diagrams considered cannot be treated as free particles as would be the case in the asymptotic region $Q^2 \gg \Lambda_c^2$. An appropriate treatment should deal with quarks as states

which are confined in the nucleon. Due to the lack of a rigorous theory for confinement in QCD one has to engage phenomenological models. In this work we are using the perturbative chiral quark model (PCQM) [13,14] treating quarks as extended objects, the constituent quarks, which are confined in the nucleon. In this model each quark vertex acquires a form factor with the characteristic momentum scale $\Lambda_c \sim 1 \text{ GeV}$ related to the confinement length $l_c \sim \Lambda_c^{-1}$. In the diagrams of Fig. 1 these form factors set the scale for the loop momentum q_ν of the virtual neutrino. This is in contrast to the previous analysis [3] of the diagrams Fig. 1a,b associated with different (neutrino mass dependent) terms of the (μ^-, e^-) conversion amplitude, where the q_ν scale is set by the W-boson mass due to the presence of the corresponding propagators in these diagrams.

Knowing the characteristic scale $q_0 \sim \Lambda_c$ of the neutrino momentum q_ν in the diagrams of Fig. 1, we consider the general structure of the (μ^-, e^-) conversion amplitude $\mathcal{A}_{\mu e}$. In the (ν_i, ν_h) neutrino scenario introduced above one can write

$$\begin{aligned} \mathcal{A}_{\mu e} &\sim \int \left(\sum_i \frac{U_{\mu i} U_{ei}^*}{q^2 - m_i^2 + i\epsilon} \right) \cdot G(q^2/q_0^2) d^4 q \quad (3) \\ &\sim \int \frac{1}{q^2} \sum_i^{light} U_{\mu i} U_{ei}^* \left(1 + \frac{m_i^2}{q^2} \dots \right) \cdot G(q^2/q_0^2) d^4 q - \frac{U_{\mu h} U_{eh}^*}{m_h^2} \int G(q^2/q_0^2) d^4 q \quad (m_h \gg q_0). \end{aligned}$$

Here $G(q^2/q_0^2)$ is a characteristic function suppressing the contribution for $q^2 \gg q_0^2$ in the loop momentum integration. Then it follows that

$$\mathcal{A}_{\mu e} \approx \begin{cases} \left(\sum_i U_{\mu i} U_{ei}^* \frac{m_i^2}{q_0^2} \right) \int \frac{q_0^2}{q^2} G(q^2/q_0^2) \frac{d^4 q}{q^2}, & \text{for } m_h \ll q_0 \\ -U_{\mu h} U_{eh}^* \int G(q^2/q_0^2) \frac{d^4 q}{q^2} & \text{for } m_h \gg q_0 \end{cases} \quad (4)$$

as a consequence of the unitarity of the mixing matrix with $\sum_i U_{\mu i} U_{ei}^* = 0$.

Previously, only the case $m_h \ll q_0$ of Eq. (4) was considered in the literature [3,5,15]. Because of the smallness of the ratio m_i^2/q_0^2 the neutrino exchange mechanism leads to rates for the (μ^-, e^-) conversion which are out of reach for ongoing and near future experiments. The situation changes if there exists a heavy neutrino state ν_h with mass $m_h \gg q_0$ and with a non-vanishing admixture of active flavors $\nu_{\mu, e}$. In this case the suppression factor associated with the small neutrino masses is replaced by the product of mixing matrix

elements $U_{\mu h}U_{eh}^*$ as indicated in Eq. (4). Since the existing experimental constraints on $U_{\mu h}U_{eh}^*$ are not stringent [16] one may expect much larger rates for (μ^-, e^-) conversion in the (ν_l, ν_h) scenario than for the case without an intermediate mass ν_h state.

Following the standard approach [7] we consider the effective nucleon Lagrangian written as

$$\begin{aligned} \mathcal{L}_{\mu e}^{eff.}(x) = & G_F^2 m_\mu^2 U_{\mu h}U_{eh}^* \bar{e}(x)\gamma_\alpha(1 - \gamma_5)\mu(x) \times \\ & [\bar{p}(x)\gamma^\alpha(f_V^p - f_A^p\gamma_5)p(x) + \bar{n}(x)\gamma^\alpha(f_V^n - f_A^n\gamma_5)n(x)] + h.c.. \end{aligned} \quad (5)$$

Here m_μ is the mass of the muon. The partial contributions of the diagrams Fig. 1a,b,c are contained in the coupling coefficients as $f_{V,A}^N = f_{V,A}^{N;1a} + f_{V,A}^{N;1b} + f_{V,A}^{N;1c}$. In the present work we restrict ourselves to the dominant mode of (μ^-, e^-) conversion, where the axial-vector current contribution [15] is neglected and, thus, only the vector form factors $f_V^{p,n}$ are relevant for the subsequent analysis.

We evaluated the form factors $f_V^{p,n}$ within the perturbative chiral quark model (PCQM), a relativistic quark model suggested in [13] and extended in [14] for the study of low-energy properties of baryons. The model operates with relativistic quark wave functions and takes into account quark confinement as well as chiral symmetry requirements. The PCQM was successfully applied to σ -term physics and to the electromagnetic properties of the nucleon [14]. In the present analysis we included the contributions from both the one-body (Fig. 1a, b) and the two-body (Fig. 1c) diagrams neglecting the external three-momenta of the leptons. For the one-body diagrams of Fig. 1a and Fig. 1b we restrict the expansion of the quark propagator to the ground state eigenmode:

$$iG_\psi(x, y) \rightarrow iG_0(x, y) = u_0(\vec{x})\bar{u}_0(\vec{y})e^{-i\mathcal{E}_0(x_0-y_0)}\theta(x_0 - y_0), \quad (6)$$

where \mathcal{E}_0 and $u_0(\vec{x})$ are the quark ground state energy and wave function; that is we restrict the intermediate baryon states to N and Δ configurations. In Ref. [14] we showed that this approximation for the quark propagator works quite well in the phenomenology of low-energy nucleon physics.

With above approximations the partial contributions of the diagrams of Fig. 1a,b,c to the coupling constant of the vector current are:

$$f_V^{N;1a} = \frac{1}{2} \int \frac{d^3k}{(2\pi)^3} \int d^3x \int d^3y e^{i\vec{k}(\vec{x}-\vec{y})} \frac{1}{|\vec{k}| - m_\mu - i\varepsilon} \quad (7)$$

$$\times \langle N | \sum_{i=1}^3 \left(\Phi_0(\vec{x}) \Phi_0(\vec{x}) + \vec{\Phi}(\vec{x}) \vec{\Phi}(\vec{x}) \right)^{(i)} | N \rangle,$$

$$f_V^{N;1b} = \frac{1}{2} \int \frac{d^3k}{(2\pi)^3} \int d^3x \int d^3y e^{i\vec{k}(\vec{x}-\vec{y})} \frac{1}{|\vec{k}| + m_\mu} \quad (8)$$

$$\times \langle N | \sum_{i=1}^3 \left(\Phi_0(\vec{x}) \Phi_0(\vec{x}) + \vec{\Phi}(\vec{x}) \vec{\Phi}(\vec{x}) \right)^{(i)} | N \rangle,$$

$$f_V^{N;1c} = \frac{1}{2} \int \frac{d^3k}{(2\pi)^3} \int d^3x \int d^3y e^{i\vec{k}(\vec{x}-\vec{y})} \left(\frac{1}{|\vec{k}| - m_\mu - i\varepsilon} - \frac{1}{|\vec{k}| + m_\mu} \right) \quad (9)$$

$$\times \langle N | \sum_{i \neq j}^3 \left(\Phi_0(\vec{x})^{(i)} \Phi_0(\vec{x})^{(j)} + \vec{\Phi}(\vec{x})^{(i)} \vec{\Phi}(\vec{x})^{(j)} \right) | N \rangle.$$

Here i and j are the quark indices, $\Phi_0(\vec{x}) = \bar{u}_0(\vec{x})\gamma_0 u_0(\vec{x})$ and $\vec{\Phi}(\vec{x}) = \bar{u}_0(\vec{x})\vec{\gamma} u_0(\vec{x})$ are the time and spatial components of the quark vector current. The single components are projected onto the three-quark state building up the nucleon state $|N\rangle$. As in Refs. [14] we use the variational *Gaussian ansatz* [17] for the quark ground state wave function given by:

$$u_0(\vec{x}) = N \exp\left[-\frac{\vec{x}^2}{2R^2}\right] \begin{pmatrix} 1 \\ i\rho \frac{\vec{\sigma}\vec{x}}{R} \end{pmatrix} \chi_s \chi_f \chi_c, \quad (10)$$

where χ_s, χ_f, χ_c refer to the spin, flavor and color spinors. The constant $N = [\pi^{3/2}R^3(1 + 3\rho^2/2)]^{-1/2}$ is fixed by the normalization condition.

Our Gaussian ansatz contains two model parameters: the dimensional parameter R and the dimensionless parameter ρ . The parameter ρ can be related to the axial coupling constant g_A calculated in zeroth-order (or 3q-core) approximation:

$$g_A = \frac{5}{3} \left(1 - \frac{2\rho^2}{1 + \frac{3}{2}\rho^2} \right) = \frac{5}{3} \frac{1 + 2\gamma}{3}, \quad (11)$$

where γ is a relativistic reduction factor

$$\gamma = \frac{1 - \frac{3}{2}\rho^2}{1 + \frac{3}{2}\rho^2} = \frac{9}{10}g_A - \frac{1}{2}. \quad (12)$$

The parameter R can be physically understood as the mean radius of the three-quark core and is related to the charge radius $\langle r_E^2 \rangle_{LO}^P$ of the proton in the leading-order (or zeroth-order) approximation as [14]

$$\langle r_E^2 \rangle_{LO}^P = \frac{3R^2}{2} \frac{1 + \frac{5}{2}\rho^2}{1 + \frac{3}{2}\rho^2} = R^2 \left(2 - \frac{\gamma}{2} \right). \quad (13)$$

In our calculations we use the tree-level value $g_A=1.25$ as obtained in Chiral Perturbation Theory [18] and the averaged value of $R = 0.6$ fm [14] corresponding to $\langle r_E^2 \rangle_{LO}^P = 0.6$ fm².

A straightforward analytical evaluation of the expressions in Eqs. (7)-(9) results in the following values for the partial isospin dependent vector coupling constants:

$$\begin{aligned} f_V^{p;1a} &= 2.37 + i 0.41, & f_V^{n;1a} &= 1.19 + i 0.21, \\ f_V^{p;1b} &= 0.64, & f_V^{n;1b} &= 1.27, \\ f_V^{p;1c} &= 0.44 + i 0.14, & f_V^{n;1c} &= 0.44 + i 0.14, \end{aligned} \quad (14)$$

For the total nucleon vector coupling constants $f_V^{p,n}$, entering in Eq. (5), we finally obtain the values

$$f_V^p = 3.45 + i 0.55, \quad f_V^n = 2.90 + i 0.35, \quad (15)$$

which are just the sum of the partial contributions.

Starting from the effective Lagrangian of Eq. (5) the branching ratio of the coherent (μ^- , e^-) conversion is derived as

$$R_{\mu e} = |U_{\mu h} U_{eh}^*|^2 \frac{2}{\pi} m_\mu (G_F m_\mu^2)^4 \frac{p_e E_e}{m_\mu^2} F(Z, p_e) \frac{|\mathcal{M}_{\mu e}|^2}{\Gamma_{\mu\nu\mu}}. \quad (16)$$

Here, E_e ($E_e = m_\mu - \varepsilon_b$, ε_b is the muon binding energy) and p_e ($p_e = |\vec{p}_e|$) are energy and momentum of the outgoing electron. $F(Z, p_e)$ is the relativistic Coulomb factor [19] and the nuclear structure factor is defined as

$$\mathcal{M}_{\mu e} = \frac{1}{\sqrt{m_\mu^3}} (f_V^p \mathcal{M}_p + f_V^n \mathcal{M}_n). \quad (17)$$

In our analysis we used values for the nuclear matrix elements $\mathcal{M}_{p,n}$ as derived in Ref. [7]. Using the calculated vector coupling constants as an input, in Table I we indicate the

numerical values for the relevant quantities entering in Eq. (16). With these values we get the following results for the coherent (μ^- , e^-) conversion on the nuclear targets ^{48}Ti , ^{197}Au and ^{27}Al as:

$$\frac{R_{\mu e}^{theor}}{|U_{\mu h}U_{eh}^*|^2} = 3.19 \times 10^{-11} (^{27}\text{Al}), \quad 6.34 \times 10^{-11} (^{48}\text{Ti}), \quad 4.73 \times 10^{-10} (^{197}\text{Au}), \quad (18)$$

which is valid for a heavy neutrino state ν_h with mass $m_h \gg \Lambda_c \sim 1$ GeV. From these results we derive upper limits on the product of mixing matrix elements $|U_{\mu h}U_{eh}^*|$ which correspond to the sensitivity of present and near future experiments discussed in the introduction. These limits which are set by the experimental upper bounds are listed in Table II. The present constraint $|U_{\mu h}U_{eh}^*| \leq 0.1$, provided by the SINDRUM II ^{48}Ti experiment, is rather weak. An improvement on this bound is expected from the ongoing SINDRUM II ^{197}Au experiment. Significant sensitivity, down to $10^{-4} - 10^{-3}$, will be hopefully achieved by the future MECO (target ^{27}Al) and PRIME (target ^{48}Ti) experiments.

The mixing of massive neutrinos, like ν_h with active $\nu_{e,\mu,\tau}$ flavors was previously looked for in various experiments except for (μ^- , e^-) conversion. An extensive list for the constraints on the $|U_{eh}|$ and $|U_{\mu h}|$ mixing matrix elements for various masses m_h is given in Ref. [16]. For $m_h \leq 19.6$ GeV all the values of $|U_{\mu h}|$ and $|U_{eh}|$ have been excluded by the MARK II collaboration. The ALEPH collaboration ruled out all values of these matrix elements for $25.0 \leq m_h \leq 42.7$ GeV. However, above 42.7 GeV there exist only narrow domains of m_h where $|U_{\alpha h}|$, with $\alpha = e, \mu$, are constrained. The typical constraints are $|U_{\alpha h}|^2 \leq 10^{-10} - 10^{-5}$. The (μ^- , e^-) conversion constraints in Table II cover the partially constrained region $m_h \geq 42.7$ GeV and extend into the region $m_h \geq 1600$ GeV currently unconstrained. On the other hand, the poorly explored region $m_h \geq 42.7$ GeV offers a loop-hole for observation of the (μ^- , e^-) conversion in future experiments as its rate is unconstrained in the most part of this mass region.

In summary, we have studied the non-photonic neutrino exchange mechanism of coherent (μ^- , e^-) conversion in nuclei in the presence of sterile neutrinos. We found a new tree level contribution to the (μ^- , e^-) conversion (Fig. 1c) which is as important as the previously

known box-type contributions (Fig. 1a,b). The nucleon form factors, parameterizing the effective nucleon Lagrangian, have been analyzed within the perturbative chiral quark model [14]. In this model the momentum scale of the virtual neutrino is set by the quark confinement with $\Lambda_c \sim 1$ GeV in the three diagrams. This significantly differs from the previous analysis [3] of the diagrams Fig. 1a,b where this scale is of the order of $\sim M_W$. The lowering the neutrino momentum scale has a notable effect on the analysis of the observability of the (μ^-, e^-) conversion. We have shown that in the neutrino scenario with at least one heavy neutrino state ν_h with mass $m_h \gg \Lambda_c \sim 1$ GeV the rate of this lepton flavor violating process could be large enough to be observed in planned experiments. This observation is in contrast to the conventional belief that (μ^-, e^-) conversion will not be detected experimentally even in the distant future if the process is dominated by the neutrino mechanism. It turns we derived new upper bounds on the product of ν_h neutrino mixing matrix elements from the non-observation of this process in running and planned experiments.

Acknowledgements. This work was supported by the Deutsche Forschungsgemeinschaft (DFG, grants FA67/25-1 and 436 SLK 17/298.) and in part by Fondecyt (Chile) under grant 8000017, by a Cátedra Presidencial (Chile) and by RFBR (Russia) under grant 00-02-17587.”

REFERENCES

- [1] Super-Kamiokande Coll., S. Fukuda *et al.*, Phys. Rev. Lett. **85**, 3999 (2000); Phys. Rev. Lett. **86**, 5651 (2001).
- [2] Q.R. Ahmad *et al.*, <http://www.sno.phy.queensu.ca/>, nucl-ex/0106015.
- [3] T.S. Kosmas, G.K. Leontaris, and J.D. Vergados, Prog. Part. Nucl. Phys. **33**, 397 (1994).
- [4] W.J. Marciano, Lepton flavor violation, summary and perspectives, Summary talk in the conference on “New initiatives in lepton flavor violation and neutrino oscillations with very intense muon and neutrino beams”, Honolulu-Hawaii, USA, October 2-6, 2000, http://meco.ps.uci.edu/lepton_workshop.
- [5] T.S. Kosmas, Amand Faessler, and J.D. Vergados, J. Phys. **G 23**, 693 (1997).
- [6] A. Faessler, T.S. Kosmas, S.G. Kovalenko, and J.D. Vergados, Nucl. Phys. **B 587**, 25 (2000).
- [7] T.S. Kosmas, S. Kovalenko, and I. Schmidt, Phys. Lett. **B 511**, 203 (2001); Phys.Lett. **B 519**, 78 (2001).
- [8] T.S. Kosmas, A. Faessler, F. Šimkovic, and J.D. Vergados, Phys. Rev. **C 56**, 526 (1997).
- [9] SINDRUM II Coll., C. Dohmen *et al*, Phys. Lett. **B 317**, 631 (1993); W. Honecker *et al*, Phys. Rev. Lett. **76**, 200 (1996); P. Wintz, Status of Muon Electron Conversion at PSI, Invited talk at [4].
- [10] MECO Collaboration, J.L. Popp hep-ex/0101017, J. Sculli, The MECO experiment, Invited talk at [4].
- [11] The homepage of the PRISM project: <http://www-prism.kek.jp>; Y. Kuno, Lepton Flavor Violation Experiments at KEK/JAERI Joint Project of High Intensity Proton Machine, in Proceedings of Workshop of “LOWNU/NOON 2000”, Tokyo, December 4-8, 2000.

- [12] C. Dib, V. Gribov, S. Kovalenko, I. Schmidt, Phys. Lett. B **493**, 82 (2000); V. Gribov, S. Kovalenko, I. Schmidt, Nucl. Phys. B (2001), hep-ph/0102155.
- [13] T. Gutsche and D. Robson, Phys. Lett. B **229**, 333 (1989); T. Gutsche, Ph. D. Thesis, Florida State University, 1987 (unpublished).
- [14] V.E. Lyubovitskij, Th. Gutsche, A. Faessler, and Th. Gutsche, A. Faessler, and E.G. Drukarev, Phys. Rev. D **63** 054026 (2000); V.E. Lyubovitskij, Th. Gutsche, and A. Faessler, Phys. Rev. C **64**, 065203 (2001); V.E. Lyubovitskij, Th. Gutsche, A. Faessler, and R. Vihn Mau, Phys. Lett. **520**, 204 (2001).
- [15] J.D. Vergados, Phys. Rep. **133**, 1 (1986).
- [16] D.E. Groom et al., The European Physical Journal C **15**, 1 (2000).
- [17] I. Duck, Phys. Lett. B **77**, 223 (1978).
- [18] J. Gasser, M. E. Sainio, and A. B. Švarc, Nucl. Phys. B **307**, 779 (1988).
- [19] M. Doi, T. Kotani, and E. Takasugi, Prog. Theor. Phys., Suppl. **83**, 1 (1985).
- [20] T. Suzuki, D. Mearsday and J. Roalsvig, Phys. Rev. C **35**, 236 (1987).

TABLES

TABLE I. The nuclear structure factor $\mathcal{M}_{\mu e}$ (dimensionless) and other quantities of Eq. (16). The experimental values of the total muon capture rate $\Gamma_{\mu\nu\mu}$ are from Ref. [20].

Nucleus	$p_e (fm^{-1})$	$\epsilon_b (MeV)$	$\Gamma_{\mu\nu\mu} (\times 10^6 s^{-1})$	$F(Z, p_e)$	$ \mathcal{M}_{\mu e} $
^{27}Al	0.531	-0.470	0.71	1.37	0.754
^{48}Ti	0.529	-1.264	2.60	1.62	1.87
^{197}Au	0.485	-9.938	13.07	3.91	7.37

TABLE II. Upper bounds on the product of mixing matrix elements $|U_{\mu h}U_{eh}^*|$ of a heavy neutrino ν_h with $\nu_{e,\mu}$ flavors in the mass region $m_h \gg 1$ GeV as derived from the sensitivity of present and near future (μ^-, e^-) conversion experiments.

Nucleus	Present limits			Expected limits		
	$R_{\mu e}^{exp.}$	Ref.	$ U_{\mu h}U_{eh}^* $	$R_{\mu e}^{exp.}$	Ref.	$ U_{\mu h}U_{eh}^* $
^{27}Al				$< 5 \times 10^{-17}$	[10]	$< 1.2 \times 10^{-3}$
^{48}Ti	$< 6.1 \times 10^{-13}$	[9]	$< 9.8 \times 10^{-2}$	$< 1 \times 10^{-18}$	[11]	$< 1.3 \times 10^{-4}$
^{197}Au	$< 2.0 \times 10^{-11}$	[9]	< 0.21	$< 6 \times 10^{-13}$	[9]	$< 3.5 \times 10^{-2}$

FIGURES

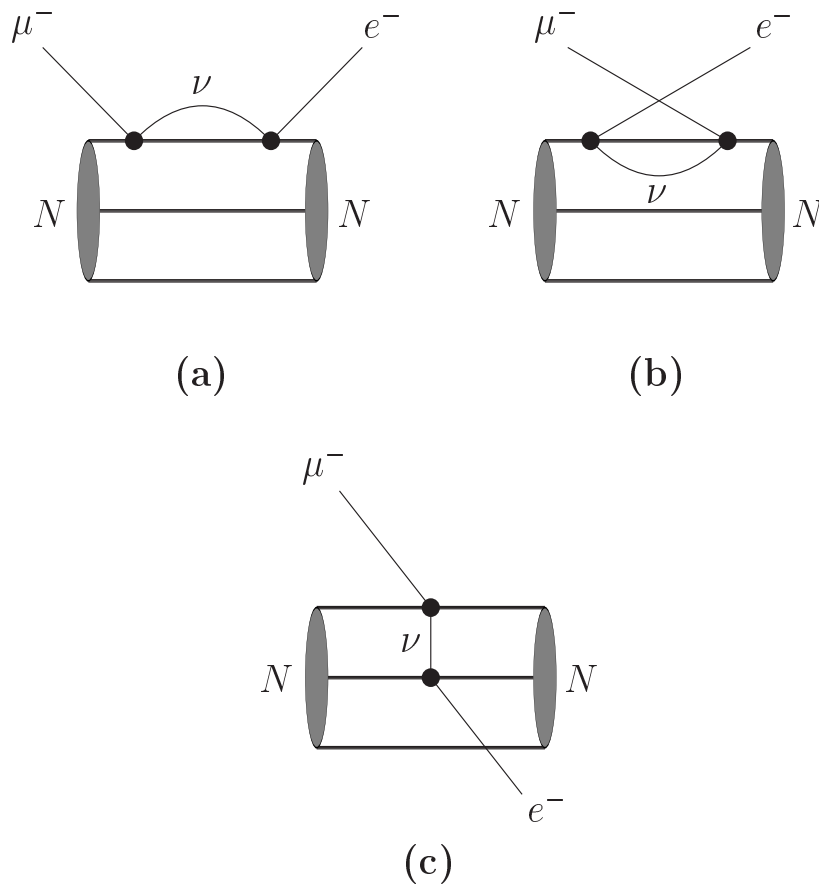


FIG. 1. Feynman diagrams for (μ^-, e^-) conversion in nuclei associated with neutrino exchange on the quark level. Both one- (a,b) and two-body (c) mechanisms are considered.